SUPPLEMENTARY INFORMATION

Supplementary Methods

Supplementary Table SI
Yeast strains and plasmids used in this study

Supplementary Figure S1
Separation of two species of tubulin dimers by Mono Q anion-exchange column chromatography

Supplementary Figure S2
Distributions of run length and velocity in single-molecule motility assay

Supplementary Figure S3
Distributions of unbinding force and stall force

Supplementary Figure S4
Relationship between unbinding force and stall force

Supplementary Figure S5
Simultaneous observation of Cy3-labeled HK560 and unlabeled MT

Supplementary Methods

Construction of mutant strains and growth conditions

As the aim of our study was to examine the motility of kinesin along mutated MTs, it was necessary to obtain yeast MTs that were stable in the low concentrations required for in vitro motility assay (~10 μg/ml). For that purpose, Taxol-binding ability was introduced into a β-tubulin gene by site-directed mutagenesis at five amino acids (Gupta et al, 2003) and the gene *tub2-A19K-T23V-G26D-N227H-Y270F* thus obtained was referred to as $TUB2^{tax}$. The yeast strain expressing *TUB1* and $TUB2^{tax}$ (SUY104) was used as the wild type.

To construct mutants, site-directed mutagenesis in the sequence coding for the MT outer surface region, from α-helix 11 to 12 (H11-12) in both α- and β-tubulin, was performed by polymerase chain reaction (PCR) using the overlap extension method (Ho et al, 1989). The plasmids and mutant strains used in this study are listed in Supplementary Table SI. To test the viability of the yeast strains with the charged-to-alanine mutations, we first used the plasmid shuffle method (Boeke et al, 1984) with the *TUB1* and *TUB2* shuffle strain SUY57. Consequently, slow growth was achieved by the mutations α-D393A, E415A, E421A and β-E421A in the mutant strains SUY192, SUY197, SUY109 and SUY121, respectively.

The mutated tubulin that led to the inviability of cells in this test was co-expressed under the *GAL10* promoter with harmless tubulin containing numerous negatively-charged amino acids at the C-terminus (Tub1p_plusE [for α-tubulin lethal mutants] or $Tub2^{tax}$p_plusE [for β-tubulin lethal mutants]). The only exception was the SUY213 (β-R380A) strain, since the tubulin dimer containing β-R380A tubulin has an unusual elution profile in Mono Q columns; this strain was co-expressed with harmless β-tubulin with a truncated C-terminus ($Tub2^{tax}$p_minusE). In either case, tubulin dimers composed of harmless tubulin were biochemically separated from dimers composed of lethal tubulin in the purification process (Supplementary Figure S1). The mutant strains thus constructed are SUY207, SUY208, SUY209, SUY210, SUY213, SUY212, SUY152 and SUY153 for α-D397A, R403A, E416A, E418A, β-R380A, E407A, E410A and D417A, respectively.

All strains were first cultured in YPD medium containing 2 % glucose (Sherman, 1991) at 30˚C until cell growth reached the late-log phase. Thereafter, the SUY207, SUY208, SUY209, SUY210, SUY213, SUY212, SUY152 and SUY153 strains were transferred to YPG medium containing 3 % galactose and were cultured for another 8 h to induce the expression of tubulin with lethal mutations (Burke et al, 1989).

Purification of tubulin from yeast cell lysate

Purification of tubulin was performed based on our original protocol (Uchimura et al, 2006), with some revisions at a particular step of MT polymerization. Cells collected from 6 L of culture (~40 g wet weight) were disrupted in PME buffer (100 mM piperazine-N, N'-bis(2-ethanesulfonic acid) (PIPES), 10 mM MgSO4, 2 mM EGTA, 1 mM GTP; pH 6.8) using a French pressure cell (Model 5501; Ohtake works Co.) and the cell lysate (15-20 mg/ml of soluble protein in a total volume of ~80 ml) was incubated for 30 min with 6 ml of DEAE-Sepharose resin (DEAE Sepharose Fast Flow, GE Healthcare). The resin was loaded into an empty column, washed with PME buffer containing 0.06 M NaCl, and eluted with the same buffer containing 0.25 M NaCl. This crude tubulin fraction was diluted three-fold with PME buffer and further fractionated by FPLC on a Mono Q column (HR 10/10, GE Healthcare) through a 0.1-1.0 M NaCl gradient. Depending on the net charge of the tubulin dimer, tubulin was eluted between 0.2 and 0.4 M NaCl (Supplementary Figure S1). Only the major fraction was collected, concentrated to approximately 15 mg/ml by ultra-filtration (Amicon Ultra-15 Centrifugal Filter Devices, Millipore), and polymerized into MTs in the presence of 1 μM Taxol at 30˚C for 15 min. Then, the Taxol concentration was increased to 20 μM to elongate and stabilize the MTs. The polymerized MTs were centrifuged through a glycerol cushion and the pellet was washed twice with washing buffer containing 2 mM ATP (composition of the washing buffer for the first round of centrifugation is 1 M NaCl, 80 mM PIPES, 5 mM $MgCl_2$, 1 mM EGTA, pH 6.8, 2 mM ATP, 1 mM GTP, and 20 μM Taxol; for the second round of centrifugation, the same buffer is used without NaCl). The pellet after the second centrifugation was suspended in 50-100 μl of x2 MA buffer (20 mM PIPES, 10 mM Kacetate, 4 mM $MgSO_4$, 2 mM EGTA, 0.2 mM EDTA; pH 6.8) containing 1 mM GTP and 20 μM Taxol. This revised protocol generated 300~500 μg of tubulin from 6 L of culture with a purity above 95 % on SDS gel electrophoresis. The MTs can be stably stored on ice for more than 2 weeks and are used for experimentation within 1 week after purification.

Supplementary References

Boeke JD, LaCroute F, Fink GR (1984) A positive selection for mutants lacking orotidine-5'-phosphate decarboxylase activity in yeast: 5-fluoro-orotic acid resistance. *Mol Gen Genet* **197**(2)**:** 345-346

Burke D, Gasdaska P, Hartwell L (1989) Dominant effects of tubulin overexpression in Saccharomyces cerevisiae. *Mol Cell Biol* **9**(3)**:** 1049-1059

Gupta ML, Jr., Bode CJ, Georg GI, Himes RH (2003) Understanding tubulin-Taxol interactions: mutations that impart Taxol binding to yeast tubulin. *Proc Natl Acad Sci U S A* **100**(11)**:** 6394-6397

Ho SN, Hunt HD, Horton RM, Pullen JK, Pease LR (1989) Site-directed mutagenesis by overlap extension using the polymerase chain reaction. *Gene* **77**(1)**:** 51-59

Sherman F (1991) Getting started with yeast. *Methods Enzymol* **194:** 3-21

Uchimura S, Oguchi Y, Katsuki M, Usui T, Osada H, Nikawa J, Ishiwata S, Muto E (2006) Identification of a strong binding site for kinesin on the microtubule using mutant analysis of tubulin. *EMBO J* **25**(24)**:** 5932-5941

Supplementary Table SI Yeast strains and plasmids used in this study

Designation	Description	Reference
Yeast Strains		
YPH499	*MATa, ura3-52, lys2-801, ade2-101, trp1-Δ63, his3-Δ200, leu2-Δ1*	Ref. (1)
SUY57	*MATa, ura3-52, lys2-801, ade2-101, trp1-Δ63, his3-Δ200, leu2-Δ1, tub1::natNT2, tub2::hphMX4, tub3::ADE2, pSU205*	Ref. (2)
SUY104	*MATa, ura3-52, lys2-801, ade2-101, trp1-Δ63, his3-Δ200, leu2-Δ1, tub1::natNT2, tub2::hphMX4, tub3::ADE2, pSU207, pSU251*	Ref. (2)
SUY192	*MATa, ura3-52, lys2-801, ade2-101, trp1-Δ63, his3-Δ200, leu2-Δ1, tub1::natNT2, tub2::hphMX4, tub3::ADE2, pSU209, pSU458*	This study
SUY197	*MATa, ura3-52, lys2-801, ade2-101, trp1-Δ63, his3-Δ200, leu2-Δ1, tub1::natNT2, tub2::hphMX4, tub3::ADE2, pSU209, pSU465*	This study
SUY109	*MATa, ura3-52, lys2-801, ade2-101, trp1-Δ63, his3-Δ200, leu2-Δ1, tub1::natNT2, tub2::hphMX4, tub3::ADE2, pSU209, pSU219*	This study
SUY121	*MATa, ura3-52, lys2-801, ade2-101, trp1-Δ63, his3-Δ200, leu2-Δ1, tub1::natNT2, tub2::hphMX4, tub3::ADE2, pSU207, pSU240*	Ref. (2)
SUY147	*MATa, ura3-52, lys2-801, ade2-101, trp1-Δ63, his3-Δ200, leu2-Δ1, tub1::natNT2, tub2::hphMX4, tub3::ADE2, pSU277, pSU209*	This study
SUY148	*MATa, ura3-52, lys2-801, ade2-101, trp1-Δ63, his3-Δ200, leu2-Δ1, tub1::natNT2, tub2::hphMX4, tub3::ADE2, pSU207, pSU278*	Ref. (2)
SUY187	*MATa, ura3-52, lys2-801, ade2-101, trp1-Δ63, his3-Δ200, leu2-Δ1, tub1::natNT2, tub2::hphMX4, tub3::ADE2, pSU207, pSU428*	This study
SUY207	*MATa, ura3-52, lys2-801, ade2-101, trp1-Δ63, his3-Δ200, leu2-Δ1, tub1::natNT2, tub2::hphMX4, tub3::ADE2, pSU277, pSU209, LEU2::GAL10pro-TUB1-D397A-GAL10pro-tub2tax*	This study
SUY208	*MATa, ura3-52, lys2-801, ade2-101, trp1-Δ63, his3-Δ200, leu2-Δ1, tub1::natNT2, tub2::hphMX4, tub3::ADE2, pSU277, pSU209, LEU2::GAL10pro-TUB1-R403A-GAL10pro-tub2tax*	This study
SUY209	*MATa, ura3-52, lys2-801, ade2-101, trp1-Δ63, his3-Δ200, leu2-Δ1, tub1::natNT2, tub2::hphMX4, tub3::ADE2, pSU277, pSU209, LEU2::GAL10pro-TUB1-E416A-GAL10pro-tub2tax*	This study
SUY210	*MATa, ura3-52, lys2-801, ade2-101, trp1-Δ63, his3-Δ200, leu2-Δ1, tub1::natNT2, tub2::hphMX4, tub3::ADE2, pSU277, pSU209, LEU2::GAL10pro-TUB1-E418A-GAL10pro-tub2tax*	This study
SUY211	*MATa, ura3-52, lys2-801, ade2-101, trp1-Δ63, his3-Δ200, leu2-Δ1, tub1::natNT2, tub2::hphMX4, tub3::ADE2, pSU207, pSU278, LEU2::GAL10pro-TUB1-GAL10pro-tub2^{tax}-R380A*	This study
SUY212	*MATa, ura3-52, lys2-801, ade2-101, trp1-Δ63, his3-Δ200, leu2-Δ1, tub1::natNT2, tub2::hphMX4, tub3::ADE2, pSU207, pSU278, LEU2::GAL10pro-TUB1-GAL10pro-tub2^{tax}-E407A*	This study
SUY152	*MATa, ura3-52, lys2-801, ade2-101, trp1-Δ63, his3-Δ200, leu2-Δ1, tub1::natNT2, tub2::hphMX4, tub3::ADE2, pSU207, pSU278, LEU2::GAL10pro-TUB1-GAL10pro-tub2^{tax}-E410A*	Ref. (2)
SUY153	*MATa, ura3-52, lys2-801, ade2-101, trp1-Δ63, his3-Δ200, leu2-Δ1, tub1::natNT2, tub2::hphMX4, tub3::ADE2, pSU207, pSU278, LEU2::GAL10pro-TUB1-GAL10pro-tub2^{tax}-D417A*	Ref. (2)
SUY213	*MATa, ura3-52, lys2-801, ade2-101, trp1-Δ63, his3-Δ200, leu2-Δ1, tub1::natNT2, tub2::hphMX4, tub3::ADE2, pSU207, pSU428, LEU2::GAL10pro-TUB1-GAL10pro-tub2^{tax}-R380A*	This study
Plasmids		
pRS305	*LEU2*-based integration plasmid	Ref. (1)
pRS313	*HIS3*-based CEN plasmid	Ref. (1)
pRS314	*TRP1*-based CEN plasmid	Ref. (1)
pRS315	*LEU2*-based CEN plasmid	Ref. (1)
pRS316	*URA3*-based CEN plasmid	Ref. (1)
pSU205	pRS316 carrying *TUB1* and *TUB2*	Ref. (2)
pSU207	pRS314 carrying *TUB1*	Ref. (2)
pSU209	pRS314 carrying *TUB2tax*[a]	Ref. (2)
pSU211	pRS315 carrying *TUB1*	Ref. (2)
pSU251	pRS315 carrying *TUB2^{tax}*	Ref. (2)
pSU455	pRS315 carrying *tub1-E387A*	This study
pSU456	pRS315 carrying *tub1-K390A*	This study
pSU457	pRS315 carrying *tub1-R391A*	This study
pSU458	pRS315 carrying *tub1-D393A*	This study
pSU459	pRS315 carrying *tub1-R394A*	This study
pSU460	pRS315 carrying *tub1-R395A*	This study

pSU461	pRS315 carrying *tub1-D397A*	This study
pSU462	pRS315 carrying *tub1-K402A*	This study
pSU463	pRS315 carrying *tub1-R403A*	This study
pSU464	pRS315 carrying *tub1-E412A*	This study
pSU465	pRS315 carrying *tub1-E415A*	This study
pSU466	pRS315 carrying *tub1-E416A*	This study
pSU467	pRS315 carrying *tub1-E418A*	This study
pSU219	pRS315 carrying *tub1-E421A*	This study
pSU220	pRS315 carrying *tub1-R423A*	This study
pSU221	pRS315 carrying *tub1-E424A*	This study
pSU222	pRS315 carrying *tub1-D425A*	This study
pSU223	pRS315 carrying *tub1-E430A*	This study
pSU224	pRS315 carrying *tub1-R431A*	This study
pSU225	pRS315 carrying *tub1-D432A*	This study
pSU486	pRS315 carrying *tub1-E435A*	This study
pSU468	pRS315 carrying $tub2^{tax}$*-E376A*	This study
pSU469	pRS315 carrying $tub2^{tax}$*-K379A*	This study
pSU470	pRS315 carrying $tub2^{tax}$*-R380A*	This study
pSU471	pRS315 carrying $tub2^{tax}$*-D383A*	This study
pSU472	pRS315 carrying $tub2^{tax}$*-K390A*	This study
pSU473	pRS315 carrying $tub2^{tax}$*-R391A*	This study
pSU474	pRS315 carrying $tub2^{tax}$*-K392A*	This study
pSU475	pRS315 carrying $tub2^{tax}$*-E401A*	This study
pSU476	pRS315 carrying $tub2^{tax}$*-D404A*	This study
pSU477	pRS315 carrying $tub2^{tax}$*-E405A*	This study
pSU478	pRS315 carrying $tub2^{tax}$*-E407A*	This study
pSU237	pRS315 carrying $tub2^{tax}$*-E410A*	Ref. (2)
pSU238	pRS315 carrying $tub2^{tax}$*-E412A*	Ref. (2)
pSU239	pRS315 carrying $tub2^{tax}$*-D417A*	Ref. (2)
pSU240	pRS315 carrying $tub2^{tax}$*-E421A*	Ref. (2)
pSU277	pRS313 carring *tub1-plusE*[b]	This study
pSU278	pRS313 carring $tub2^{tax}$*-plusE*[c]	Ref. (2)
pSU428	pRS313 carring $tub2^{tax}$*-minusE*[d]	This study
pSU479	pRS305 carrying *GAL10pro-TUB1-D397A-GAL10pro-*$tub2^{tax}$	This study
pSU480	pRS305 carrying *GAL10pro-TUB1-R403-GAL10pro-*$tub2^{tax}$	This study
pSU481	pRS305 carrying *GAL10pro-TUB1-E416A-GAL10pro-*$tub2^{tax}$	This study
pSU482	pRS305 carrying *GAL10pro-TUB1-E418A-GAL10pro-*$tub2^{tax}$	This study
pSU483	pRS305 carrying *GAL10pro-TUB1-GAL10pro-*$tub2^{tax}$*-R380A*	This study
pSU484	pRS305 carrying *GAL10pro-TUB1-GAL10pro-*$tub2^{tax}$*-E407A*	This study
pSU342	pRS305 carrying *GAL10pro-TUB1-GAL10pro-*$tub2^{tax}$*-E410A*	Ref. (2)
pSU345	pRS305 carrying *GAL10pro-TUB1-GAL10pro-*$tub2^{tax}$*- D417A*	Ref. (2)

[a] $TUB2^{tax}$*; tub2-A19K-T23V-G26D-N227H-Y270F*

[b] *tub1-plusE; tub1-*^{440}*SYAEEEEGEEEEGEEEEGEEEEGEEEEF*

[c] $tub2^{tax}$*-plusE; tub2*^{tax}*-*^{440}*GDFGEEEEGEEEEGEEEEGEEEEGEEEEA*

[d] $tub2^{tax}$*-minusE; tub2*^{tax}*-*^{428}*ATVED*

References

1. Sikorski RS, and Hieter P (1989) A system of shuttle vectors and yeast host strains designed for efficient manipulation of DNA in *Saccharomyces cerevisiae*. Genetics *122*, 19-27

2. Uchimura, S., Oguchi, Y., Katsuki, M., Usui, T., Osada, H., Nikawa, J., Ishiwata, S., and Muto, E. (2006). Identification of a strong binding site for kinesin on the microtubule using mutant analysis of tubulin. EMBO J *25*, 5932-5941.

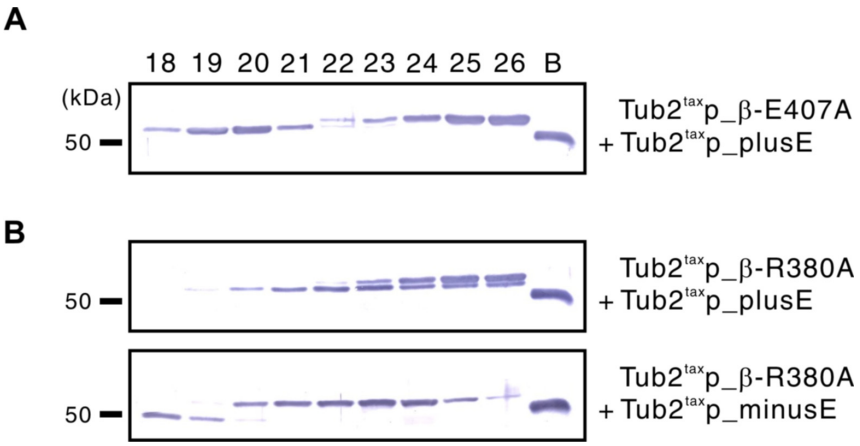

Supplementary Figure S1 Separation of two species of tubulin dimers by Mono Q anion-exchange column chromatography

An elution profile of the Mono Q column for the purification of tubulin dimers containing (**A**) β-E407A tubulin and (**B**) β-R380A tubulin. In each case, the DEAE-sepharose-purified crude tubulin fraction obtained from the yeast cell lysate was further fractionated on a Mono Q column, and each of the fractions eluted at 0.21-0.38M NaCl (fractions no. 18-26) were analyzed by Western blotting probed with anti-β-tubulin antibody.

(**A**) In the case of the β-E407A mutant, the tubulin dimers containing Tub2^{tax}p-E407A and Tub2^{tax}p-plusE were eluted separately in the fractions centred at no. 20 and 25, respectively.

(**B**) In the case of the β-380A mutant, the dimer containing Tub2^{tax}p-R380A was co-eluted with the dimer containing Tub2^{tax}p-plusE (upper panel), but was separated from the dimer containing Tub2^{tax}p-minusE (lower panel). In the latter case, each dimer containing Tub2^{tax}p-R380A and Tub2^{tax}p-minusE was eluted in the fractions centred at nos. 23 and 18, respectively. The lane labelled as "B" contains 0.1 μg of porcine brain tubulin.

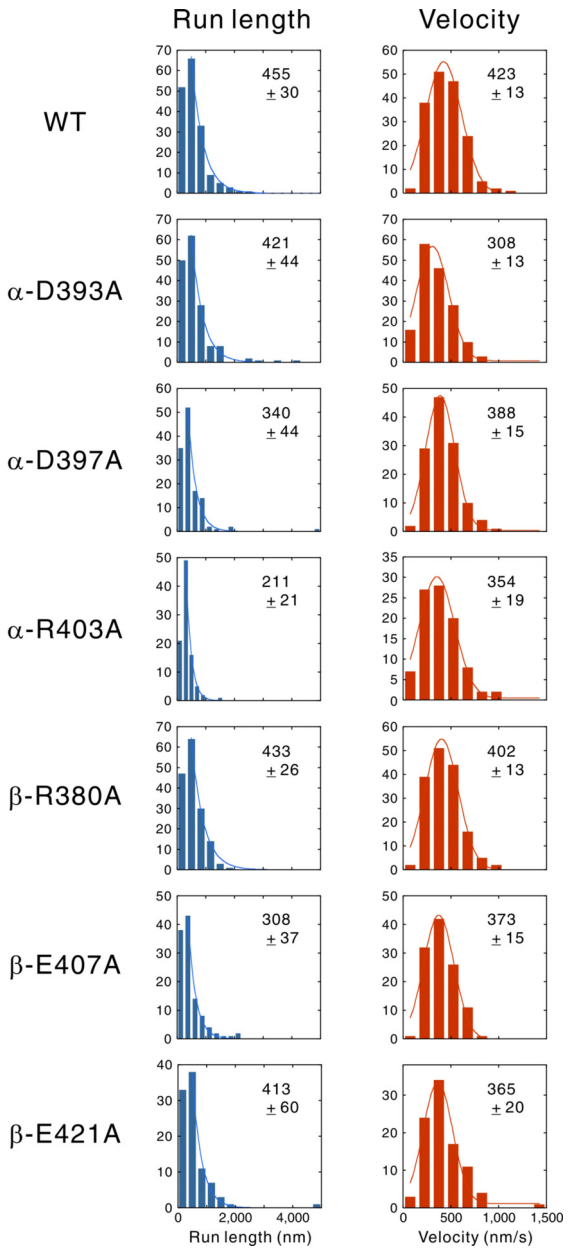

Supplementary Figure S2 Distributions of HK560 run length and velocity in single-molecule motility assay

The mean run lengths and velocities ± SEM are shown in each panel.

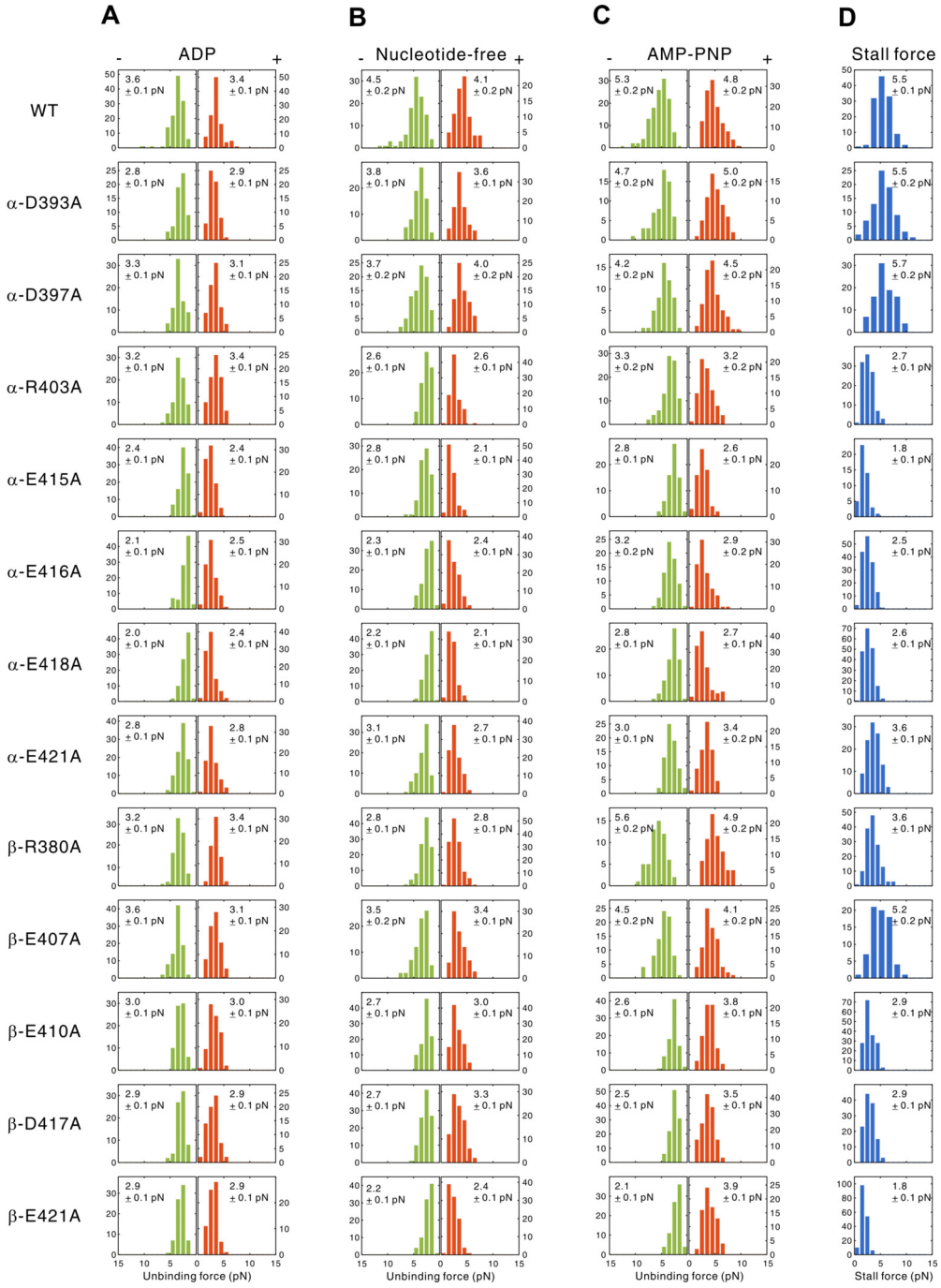

Supplementary Figure S3 Distributions of unbinding force and stall force

The distributions of the unbinding force measured for minus-end (light green) and plus-end (orange) loading directions in the presence of ADP (**A**), in the absence of nucleotides (**B**), and in the presence of AMP-PNP (**C**), as well as the distributions of the stall force measured in the presence of ATP (**D**). The mean values ± SEM are shown in each panel.

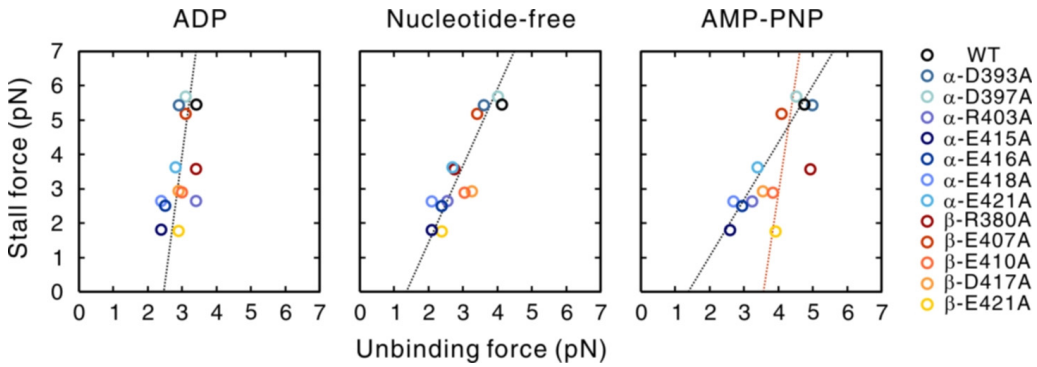

Supplementary Figure S4 Relationship between unbinding force and stall force

The stall force plotted against the unbinding force for plus-end loading measured in three nucleotide conditions. The results are quite similar to those observed for minus-end loading (Figure 3E), except for the dataset measured in the presence of AMP-PNP, where the unbinding force was virtually unaffected by mutations in β-tubulin (Uchimura et al, 2006). In the AMP-PNP state, the datasets for α- and β-tubulin mutants were independently fit by the black and red lines, respectively.

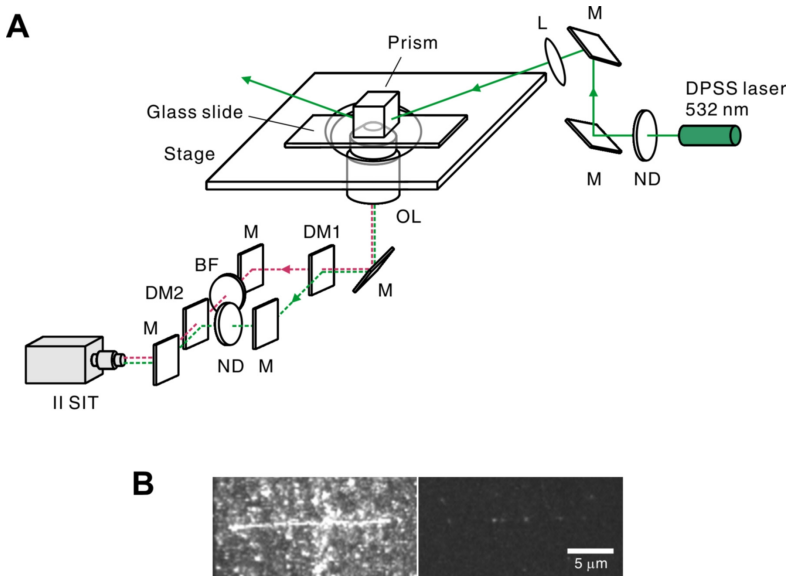

Supplementary Figure S5 Simultaneous observation of Cy3-labeled HK560 and unlabeled MT

(**A**) Schematic drawing of the optical microscope system. The images of Cy3-labeled HK560 and MT (unlabeled with the fluorescent dye) were simultaneously observed using total internal reflection fluorescence microscopy (TIRFM) based on an inverted microscope (IX-70, Olympus) with an oil-immersion objective lens (OL; PlanApo, x100, NA-1.4, Olympus). A flow chamber containing the sample was set on the microscope stage so as to make the glass slide of the chamber come into contact with the cubic quartz prism (15 x 15 x 15 mm) through a layer of pure glycerol. A DPSS laser beam (CDPS532M-050 [532 nm]; JDS Uniphase) was incident on a glass slide through a prism at an angle of 70° to normal at the quartz-to-solution interface. The beam was focused to 80 x 160 μm^2 by a lens (L), with its power 7.2 mW at the specimen plane. The fluorescence image of HK560-Cy3 and the darkfield image of MT (as a result of scattering of the incident beam) were separated using a dichroic mirror (DM1 and DM2; separation wave length of 565 nm, Chroma Technology Corp.). For the fluorescence image of Cy3, background luminescence was rejected using a barrier filter (BF; 593DF40, Semrock Inc.). For the darkfield image, the light was attenuated using a neutral density filter (ND; 1 % transmittance, Sigma Koki Co.). Both images were ultimately captured by an SIT camera (C2400-08, Hamamatsu Photonics) equipped with a Gen IV image intensifier (VS4-1845, Video Scope). M in the schematic drawing denotes mirrors.

(**B**) Darkfield image of a single MT (left) and Cy3-labeled HK560 molecules moving along the same MT (right), simultaneously displayed on the monitor. Multiple kinesin molecules are visible on the MT track.